PHYSICAL REVIEW C VOLUME 22, NUMBER 5 NOVEMBER 1980

Target fragmentation of ^{197}Au by relativistic heavy ions

S. B. Kaufman, E. P. Steinberg, B. D. Wilkins, and D. J. Henderson
Chemistry Division, Argonne National Laboratory, Argonne, Illinois 60439
(Received 19 June 1980)

The cross sections and recoil properties of a number of target fragmentation products formed by the reactions of 4.8- and 25-GeV ^{12}C and 7.6-GeV ^{20}Ne with ^{197}Au have been measured. Comparisons between these data for relativistic heavy ions and those for relativistic protons have been used to test the hypotheses of factorization and limiting fragmentation. The cross sections for most of the nuclides measured are related for different projectiles by the ratio of the total reaction cross sections. An exception is the light nuclides ($A < 30$), for which enhanced yields are found for heavy-ion projectiles compared to protons. The velocities imparted to recoil fragments by the projectiles are considerably larger for the heavy ions of $\sim 0.4\ A$ GeV than for protons, but are the same for 2.1 A GeV ^{12}C (25-GeV kinetic energy) and 28-GeV protons. Limiting fragmentation has not been reached at energies of 0.4 A GeV, as shown by the large change in recoil properties with increasing energy. The projectile kinetic energy appears to be more significant as a scaling variable than the velocity for relativistic heavy ions.

[NUCLEAR REACTIONS ^{197}Au(^{12}C, X), (^{20}Ne, X), $X = ^{24}$Na $- ^{196}$Au, $E_{^{12}C} = 4.8$ and 25 GeV, $E_{^{20}Ne} = 7.6$ GeV; measured cross sections and recoil properties; deduced mean kinetic parameters; test of factorization and limiting fragmentation.]

I. INTRODUCTION

The interactions of relativistic heavy ions with nuclei can be classified qualitatively into peripheral and central collisions.[1] A peripheral collision is one for which the impact parameter is relatively large, of the order of the sum of the nuclear radii of the target and projectile. Following a peripheral collision the projectile and target nuclei still retain much of their identity. The projectile fragment will have a charge and mass close to the initial values, generally with a loss of only a few nucleons, and will be moving with nearly the beam velocity. Similarly, the target fragment is nearly at rest in the laboratory system, and will have a relatively low excitation energy, which can be dissipated by evaporation of nucleons or, for a heavy nucleus, by fission.

In contrast to this behavior, central collisions lead to a nearly complete destruction of both nuclei. Such events, as seen in emulsion[2] or streamer chamber pictures,[1] are characterized by a large multiplicity of secondary fragments emitted at all angles, but predominantly in the forward direction. However, there is no core of projectile fragments emitted near 0° with respect to the beam direction as in a peripheral collision. The fragments formed in near-central collisions cannot be identified as coming from either target or projectile, but appear to be emitted from a system moving with a velocity intermediate between projectile and target.[2-4]

Two hypotheses originally developed to describe elementary particle interactions[5] have been found to be applicable to much of the experimental data. The hypothesis of limiting fragmentation states that at sufficiently high energies the cross sections and spectra of fragments in their proper rest frame (i.e., target or projectile) will become independent of bombarding energy. The factorization hypothesis predicts that the spectra and yield of a specific fragment may be written as a product of target and projectile factors. For a projectile fragment this implies that spectra and yield will be independent of the nature of the target, except for a total cross section term, while conversely, target fragmentation is expected to be independent of the beam.

Evidence for factorization was found for the projectile fragments of ^{12}C and ^{16}O incident on a variety of targets at energies of 1–2 A GeV.[6,7] Thus, relative isotopic yields and momentum spectra in the projectile frame were independent of the target, and were also independent of beam energy. In the case of target fragmentation there have been a number of studies of the cross sections for forming radionuclides from targets bombarded with relativistic projectiles. In a series of papers[8-10] Cumming and co-workers measured spallation cross sections for a Cu target and projectiles of protons, ^{12}C, ^{14}N, and ^{40}Ar above several GeV and found that the charge-dispersion curves were identical within errors, showing that factorization was valid for this system. In addition, the relative formation cross sections for products with a mass number greater than one-half that of the target were the same for all projectiles. Only for the lightest product

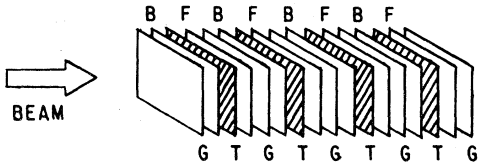

FIG. 1. Schematic diagram of the target stack. T=target foils, F=Mylar forward, B=backward catchers, G=guard foils.

nuclides, particularly ^{7}Be, was a difference found, namely larger yields with the heavy-ion projectiles than with protons.

The approach to limiting fragmentation as a function of projectile energy for spallation of Cu was demonstrated[10] by using the slope of the mass-yield curve as a measure of the mean excitation energy transferred to the target: A smaller slope corresponds to a greater mass loss, hence larger mean excitation energy. When plotted as a function of projectile kinetic energy, data for protons, ^{4}He, ^{12}C, ^{14}N, and ^{40}Ar projectiles all fell on a smooth curve, which leveled off for energies above ~3 GeV. The apparent significance of total kinetic energy, rather than velocity (or energy per nucleon), should be noted. Similar results were found for spallation of Ag,[11,12] Ta,[13,14] Au,[14,15] and Pb,[15] where multi-GeV energy protons and heavy ions were compared. In all cases the only difference in product yields was for the lightest nuclides, for which the heavy-ion yields were enhanced as compared to the proton yields. However, data for U targets[16] appear to show enhanced yields for products with $160 \leq A \leq 190$ from 25-GeV ^{12}C bombardment over those from proton bombardments. On the other hand, track detector experiments[17] have shown that the fission of Au, Bi, and U by 28-GeV ^{14}N ions is very similar, except for larger reaction cross sections, to proton-induced fission.

Further evidence on the validity of factorization and limiting fragmentation for target fragmentation products is provided by measurements of the mean ranges and forward-to-backward (F/B) ratios of the radionuclides which recoil from a thick target.[18,19] These experimental quantities can be related to the velocities imparted to the recoil fragments by two distinct reaction steps: an initial step in which the projectile imparts a forward-directed velocity $v_{\parallel}$ to the target, and a second step in which this target fragment de-excites by particle evaporation or fission to form the observed product. These two steps are formally equivalent to the abrasion-ablation model[20,21] for relativistic heavy-ion reactions.

Comparisons of these quantities[18] for 25-GeV ^{12}C and 28-GeV proton spallation of Cu showed that $v_{\parallel}$ was somewhat larger (~23%) for the heavy-ion projectile, while the second-step velocities were the same. By including data for lower energy proton and ^{4}He bombardments, a smooth decrease of $v_{\parallel}$ with increasing projectile rapidity ($y = \tanh^{-1}\beta$) was seen. From these data it appeared that limiting fragmentation was a function of projectile rapidity, or velocity, and that it had not yet been reached for 2.0 A GeV ^{12}C. The same comparison for an Au target[19] showed that the values of $v_{\parallel}$ were the same within error for 25-GeV ^{12}C and 28-GeV protons. More significantly, the values of $v_{\parallel}$ for a given nuclide did not scale with projectile rapidity, since much larger values were found for 1–3 GeV protons than for 25-GeV ^{12}C, which has comparable rapidity.

In order to investigate further the dependence of both the kinematic properties and the formation cross sections of target fragmentation products on the mass and kinetic energy of the projectile, we have made measurements for ~400 A MeV ^{12}C and ^{20}Ne interacting with an Au target. These experiments extend our previous measurement[19] with 2.1 A GeV ^{12}C to lower energies and also to a heavier projectile. The choice of Au as the target was made because of the extensive measurements we have previously made of both cross sections[22,23] and recoil properties[24–26] for a large number of nuclides formed in the interaction of protons with Au over a wide energy range. These data provide an excellent basis for comparison with heavy-ion projectiles. Measurements of thick-target recoil properties for 8.0 GeV ^{20}Ne incident on Ta have been done concurrently with the present work, and are reported separately.[27] A preliminary account of the recoil data for 25-GeV ^{12}C has been previously published.[19]

II. EXPERIMENTAL

The bombardments were done in an external beam at the LBL Bevalac, with beams of 4.8-GeV ^{12}C, 25-GeV ^{12}C, and 7.6-GeV ^{20}Ne. The targets were a stack of four Au foils, 25 mg/cm^2 thick, interspersed between 18-mg/cm^2 Mylar foils, with an arrangement as shown in Fig. 1. The purpose of this multiple-target structure was to provide a fourfold increase in total activity recoiling into the Mylar catchers over the amount which a single target-catcher stack would give. The stack was sealed in a plastic envelope under vacuum, so that atmospheric pressure held the foils in intimate contact. The ^{20}Ne bombardment was done with a number of other targets upstream; the total thickness of material through

which the beam passed was about 1.5 g/cm^2, of which about one-half consisted of heavy metals and the other half Mylar. The energy of the beam was reduced from 8.0 to 7.6 GeV by this material, and the beam was attenuated by nuclear interactions by 7%.

The beam intensity was measured with an ion chamber calibrated by the Bevalac staff[28]; fluctuations of intensity during each bombardment were recorded. Following the bombardment the four Au foils were combined to provide a single target sample. Similarly, the Mylar foils corresponding to the forward (F) and backward (B) catchers were combined to provide one F and one B set. The γ spectra of these three samples were recorded as a function of time. The details of how these spectra were resolved into individual lines and the identification and measurement of the activities of individual radionuclides are described in our previous publications.[22-25] Formation cross sections were calculated from the data using known γ-ray abundances,[22,23] together with the photopeak counting efficiences of the Ge(Li) spectrometers and the beam intensity. The activity in the F and B catchers of each nuclide was added to that in the target to calculate the cross sections.

In order to determine the effect of scattered and background radiation in the vicinity of the beam on the formation of radionuclides in the target, a portion of the target outside of the area through which the beam passed was counted. The only significant activity in that portion was that due to ^{198}Au, which is the product of the (n,γ) reaction. Assuming a uniform neutron flux was the source of this nuclide, the contribution of background neutrons to the ^{198}Au observed in the central portion of the target was estimated and subtracted from the observed activity. The result was consistent with the hypothesis that all of the ^{198}Au in the target was formed by background neutrons.

The amount of activity of other nuclides outside of the beam spot was less than 1% of that within the spot, indicating that there was no significant stray radiation other than low-energy neutrons. A different possible source of secondary radiation is that due to particles formed inside the target material. The effect of such particles has been found[14] to be negligible for targets as thin as those used here.

III. RESULTS

The results of the cross section measurements are given in Table I for each nuclide. The error given for each cross section includes the estimated error in the γ-ray decay rate, obtained from the least-squares decay curve analysis and the uncertainties in photopeak intensities after spectral analysis. The only additional error folded in was an estimated 5% uncertainty in the relative photopeak efficiency calibrations of the different Ge(Li) detectors used. Since we are primarily interested in comparing *relative* cross sections of the same nuclide formed by different projectiles, we have not included the estimated 20% uncertainty in the absolute beam intensity measurements. Such an error would cause a uniform shift in the cross section ratios when comparing the data for different projectiles.

TABLE I. Cross sections of radionuclides formed in the reactions of 4.8- and 25-GeV ^{12}C and 7.6-GeV ^{20}Ne with Au. The designation (*C*) or (*I*) for each nuclide refers to cumulative or independent cross section.

Nuclide	Cross section (mb) 4.8-GeV ^{12}C	7.6-GeV ^{20}Ne	25-GeV ^{12}C
^{24}Na (*C*)	16.7±2.2	35±6	71±10
^{28}Mg (*C*)	4.2±0.6	8.0±1.5	17.4±2.6
^{46}Sc (*I*)	7.0±0.7	9.7±1.2	15.2±1.8
^{48}V (*C*)	2.3±0.3	3.5±0.5	
^{54}Mn (*I*)	6.6±0.7	8.9±1.2	13.5±1.8
^{74}As (*I*)	4.2±0.5	4.6±0.6	5.5±0.7
^{75}Se (*C*)	7.5±0.9	9.1±1.2	13.5±2.0
^{83}Rb (*C*)	10.8±1.2	13.1±1.6	19.0±2.6
^{87}Y (*C*)	10.7±0.9	11.6±1.0	16.6±1.8
^{89}Zr (*C*)	8.9±0.7	9.9±0.9	15.8±1.7
^{90}Nb (*C*)	6.2±0.8	9.6±1.3	
^{96}Tc (*I*)	4.5±0.6	4.2±0.6	6.3±1.0
^{121}Te (*C*)	10.2±1.3	8.9±1.1	
^{127}Xe (*C*)	12.2±1.5	11.5±1.4	17.1±2.7
^{131}Ba (*C*)	14.2±1.8	16.0±3.0	16.0±3.5
^{139}Ce (*C*)	14.0±1.6	13.0±1.4	18.8±2.1
^{145}Eu (*C*)	21.3±2.5	19.7±2.3	24.4±2.6
^{146}Gd (*C*)	18.7±2.3	19.7±2.5	19.4±2.4
^{149}Gd (*C*)	22.4±2.4	19.4±2.3	23.4±3.0
^{167}Tm (*C*)	26.0±2.9	24.0±3.3	34±5
^{171}Lu (*C*)	28.8±3.4	32±4	35±5
^{175}Hf (*C*)	33±4	35±4	35±4
^{183}Re (*C*)	42±6	46±7	40±6
^{185}Os (*C*)	54±5	61±6	55±6
^{188}Pt (*C*)	51±9	54±10	
^{194}Au (*I*)	62±10	66±11	
^{196}Au (*I*)	167±15	211±18	210±20

The cross sections for many of the same nuclides listed in Table I have also been measured[14] for 8.0 GeV ^{20}Ne reacting with Au, and the results of the two different experiments are compared in Fig. 2, where the cross section ratios σ(7.6 GeV)/σ(8.0 GeV) are plotted as a function of mass number. Although there is considerable fluctuation in the ratios, the agreement between the two experiments is in general

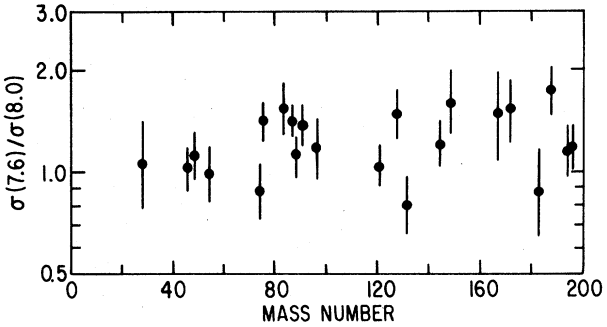

FIG. 2. Ratios of cross sections measured in this work with 7.6-GeV ^{20}Ne projectiles to those of Ref. 14 for 8.0-GeV ^{20}Ne.

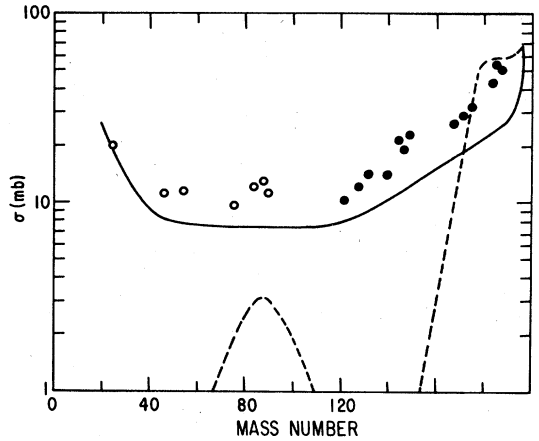

FIG. 3. Mass yield curves for different projectiles interacting with ^{197}Au. Dashed curve: 0.5-GeV p; solid curve: 6.0-GeV p; points: 4.8-GeV ^{12}C (○, calculated isobaric yield; ● observed cumulative cross section).

satisfactory. The average ratio is 1.24 ± 0.26; the deviation from unity is consistent with the uncertainties in the absolute measurement of the beam intensity. The lightest fragments tend to have a lower than average ratio, which may be due to the 5% lower beam energy, since one expects these light nuclides to have excitation functions which are still rising in this energy region, based on the proton data.[23]

The cross sections in Table I show the following main features: (1) There is a general similarity of the data for the three projectiles, in that the formation cross section of a given nuclide is about the same. The exceptions are the light nuclides ^{24}Na and ^{28}Mg, whose cross sections increase with increasing projectile energy. (2) The general pattern of the dependence of cross section on mass number is similar to that found for protons of similar kinetic energy. This is illustrated in Fig. 3, where the data for 4.8-GeV ^{12}C are compared to the mass-yield curves for protons of 0.5 and 6.0 GeV energy. The dashed curve shows how the total isobaric cross section varies with mass number for 0.5-GeV protons interacting with ^{197}Au, while the solid curve shows that variation for 6.0-GeV protons.[23]

For a proper comparison the cross sections for forming individual nuclides given in Table I must be corrected for the fraction of isobaric yield not included in the measured cross section. This correction was made by using the charge dispersion parameters derived for the proton-induced reactions.[23] For nuclides with $A \geq 121$ this correction is negligible, because the peak of the charge dispersion curve is several charge units larger than that of the typical observed product. In other words, the observed nuclides are formed almost entirely by electron-capture decay of the more neutron-deficient primary products. This is not the case for the nuclides with $A \leq 96$; in this mass region some of the observed nuclides are shielded from beta decay [those indicated by (I) in Table I], and others represent only a fraction of the total isobaric cross section. That fraction was calculated for each nuclide using the proton charge-dispersion curve,[23] and the total isobaric cross section was thus obtained. We show in Fig. 3 only those nuclides for which this correction factor was less than 2.0, i.e., the observed cross section was greater than 50% of the total. These nuclides are shown as open points in Fig. 3, while the heavier nuclides whose cumulative cross sections represent the total isobaric yield are shown as closed points.

It is clear from Fig. 3 that the mass-yield distribution for 4.8-GeV ^{12}C is similar to that of protons with about the same kinetic energy, and quite different than that of protons with about the same velocity, namely 0.5 GeV. The prominent fission peak centered at a little less than one-half the target mass which is observed for 0.5-GeV protons is absent for 0.4 A GeV ^{12}C ions, and the slope of the curve in the near-target region is much less for the heavy ions than for 0.5 GeV protons. These same features have been noted previously[13,14] for 8.0-GeV ^{20}Ne interacting with Ta and Au. In the following section we shall make more detailed comparisons of the proton-induced and heavy-ion–induced cross sections.

The results of the recoil-catcher data are expressed in terms of the fraction of each nuclide which recoils from a target of thickness W mg/cm^2 in the forward and backward directions

TABLE II. Thick-target recoil properties of radionuclides formed in the reactions of 4.8- and 25-GeV ^{12}C and 7.6-GeV ^{20}Ne with Au.

Nuclide	F/B			$2W(F+B)$ (mg/cm^2)		
	4.8-GeV ^{12}C	7.6-GeV ^{20}Ne	25-GeV ^{12}C	4.8-GeV ^{12}C	7.6-GeV ^{20}Ne	25-GeV ^{12}C
^{24}Na	4.40±0.35	5.41±0.40	1.23±0.08	18.2 ±1.2	17.0 ±1.0	12.9 ±0.8
^{28}Mg	4.38±0.40	4.74±0.45	1.22±0.12	16.1 ±1.5	15.5 ±1.3	12.6 ±1.0
^{46}Sc	3.22±0.20	3.09±0.18	1.13±0.10	8.9 ±0.7	8.5 ±0.6	7.1 ±0.5
^{48}V	3.40±0.32	3.14±0.29		8.7 ±0.6	8.1 ±0.7	
^{54}Mn	2.9 ±0.5	2.6 ±0.3	1.0 ±0.2	7.5 ±0.7	7.6 ±0.6	6.9 ±0.8
^{74}As	2.19±0.25	2.22±0.23	1.08±0.15	6.7 ±0.5	7.3 ±0.4	7.2 ±0.6
^{75}Se	2.72±0.30	2.55±0.26	1.11±0.23	6.1 ±0.6	5.7 ±0.5	5.4 ±0.6
^{83}Rb	3.20±0.40	2.67±0.30	1.04±0.12	5.5 ±0.5	5.3 ±0.5	4.7 ±0.4
^{87}Y	3.18±0.25	2.89±0.22	1.09±0.08	5.3 ±0.3	5.2 ±0.3	4.7 ±0.3
^{89}Zr	3.37±0.28	3.05±0.25	1.11±0.10	5.2 ±0.4	5.1 ±0.3	4.3 ±0.3
^{90}Nb	4.07±0.35	3.36±0.35		5.6 ±0.7	4.7 ±0.6	
^{96}Tc	3.4 ±0.5	2.9 ±0.4	1.42±0.35	4.8 ±0.6	5.3 ±0.6	3.4 ±0.6
^{139}Ce	11±4	13±4	1.40±0.30	2.04±0.15	2.71±0.20	1.53±0.15
^{145}Eu	20±10	15±5		1.79±0.18	2.13±0.20	
^{146}Gd	18±5	21±6	1.73±0.25	2.05±0.15	2.28±0.17	1.47±0.17
^{149}Gd	19±10	18±5	1.50±0.40	1.91±0.16	2.20±0.18	1.56±0.30
^{167}Tm	16±6	15±6	2.1 ±0.9	0.91±0.15	1.08±0.14	0.88±0.16

with respect to the beam, denoted by F and B, respectively. The measured values of the forward-to-backward ratio F/B, and a quantity which is approximately the mean range in the target material, $2W(F+B)$, are given in Table II.

The F/B values for 4.8-GeV ^{12}C and 7.6-GeV ^{20}Ne projectiles are similar for each nuclide, and are much larger than the F/B resulting from 25-GeV ^{12}C. This is illustrated in Fig. 4, where the 4.8-GeV ^{12}C data are compared with the data previously observed[25] with protons of 1.0, 3.0, and 28 GeV, as shown by the smooth curves. The large values of F/B indicate a large amount of forward (in the beam direction) peaking for these recoil nuclei produced with heavy ion projectiles of ~0.4 A GeV energy, but much less peaking at 2.1 A GeV. A similar but smaller decrease in F/B with increasing energy occurs with incident protons, as shown by the curves in Fig. 4. The same effect has also been observed[27] for the reactions of 8.0 GeV ^{20}Ne with Ta.

In order to analyze the recoil data presented in Table II, we use the model first proposed by Sugarman and co-workers,[29-31] and elaborated by Alexander and Winsberg.[32,33] As discussed in the Introduction, this model assumes that the nuclear reaction occurs in two distinct steps. The first step results in an excited nucleus moving forward in the laboratory system with a velocity $v_{\parallel}$, while the second step occurs on a much slower time scale, such that memory of the beam direction has been lost. The velocity resulting from the second step, V, thus must have an angular distribution which is symmetric about 90° to the beam in the moving system. In the absence of information on the angular distribution, we assume that it is isotropic in the

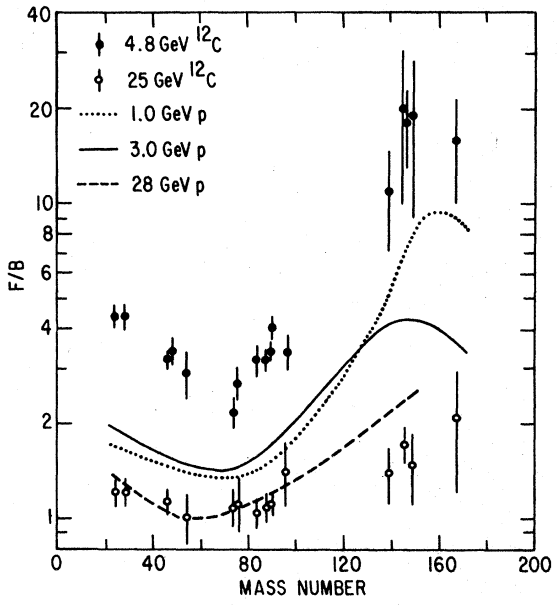

FIG. 4. Forward-to-backward ratios (F/B) for target fragments. Points are for ^{12}C projectiles at 4.8 GeV (●) and 25 GeV (○). Curves show smooth behavior of F/B for protons of 1.0, 3.0, and 28 GeV (Ref. 25).

TABLE III. Derived kinematic quantities from the two-step model analysis of recoil data. The velocity of the first step, $\beta_{\parallel} = v_{\parallel}/c$, and the momentum in the moving system arising from the second step, $P = AV$, are given.

	$10^3\beta_{\parallel}$			P (MeVA)$^{1/2}$		
	4.8-GeV ^{12}C	7.6-GeV ^{20}Ne	25-GeV ^{12}C	4.8-GeV ^{12}C	7.6-GeV ^{20}Ne	25-GeV ^{12}C
^{24}Na	18.4	19.7	2.4	46.5	44.1	42.5
^{28}Mg	17.8	18.1	2.3	49.0	47.5	46.1
^{46}Sc	10.4	9.6	1.0	50.0	47.6	43.5
^{48}V	10.9	9.6		52.1	49.1	
^{54}Mn	8.1	7.5	0.0	49.6	50.8	48.7
^{74}As	5.1	5.5	0.6	57.4	61.8	63.8
^{75}Se	5.7	5.1	0.6	53.2	50.5	50.9
^{83}Rb	5.7	4.7	0.2	51.7	50.9	48.2
^{87}Y	5.4	5.0	0.4	52.4	51.9	50.2
^{89}Zr	5.5	5.0	0.5	52.4	51.5	50.2
^{90}Nb	6.6	5.0		55.3	48.6	
^{96}Tc	4.9	4.7	1.2	51.3	56.3	42.5
^{139}Ce	4.4	5.2	0.7	36.6	41.6	38.6
^{145}Eu	4.6	4.8		33.1	37.7	
^{146}Gd	4.9	5.3	1.0	36.3	37.4	39.7
^{149}Gd	4.7	5.0	0.8	35.3	38.3	41.7
^{167}Tm	3.2	3.5	1.1	28.8	31.6	35.6

moving frame. In terms of this model, the extent of forward peaking of the recoils, as measured by F/B, arises from the forward velocity of the first step, $v_{\parallel}$. Similarly, the mean range of the recoils is primarily determined by the second step velocity V. The range-energy relationships used in the analysis were obtained for each nuclide from the tables of Northcliffe and Schilling.[34] The equations relating the experimental quantities to the model velocities are discussed by Winsberg.[33]

The results of this model analysis are given in Table III, which lists for each nuclide and projectile the calculated values of $\beta_{\parallel} \equiv v_{\parallel}/c$, and $P \equiv AV$, the momentum of the nuclide with mass number A corresponding to the velocity V. The most striking feature of these data is the considerably larger values of $\beta_{\parallel}$ found at an energy of 0.4 A GeV for both ^{12}C and ^{20}Ne than those found at 2.1 A GeV for ^{12}C. These large values of $\beta_{\parallel}$ result primarily from the large experimental F/B ratios. Their significance is discussed in the following section.

IV. DISCUSSION

A. Cross sections

The similarity between the mass-yield curves for protons above ~3 GeV and for ^{12}C and ^{20}Ne of about the same kinetic energy has been pointed out in the previous section and illustrated in Fig. 3. This similarity has been observed previously for other targets[8-14] and was interpreted as evidence that the hypothesis of limiting fragmentation was valid at these projectile energies. In the present work we are able to make a more detailed comparison of the formation cross sections of individual nuclides in the heavy-ion experiments with the proton-induced cross sections. This is because we have previously[22,23] made such proton measurements at a number of bombarding energies and thus can estimate the cross section of these nuclides at any proton energy by interpolation.

Specifically, we wish to compare these cross sections for heavy ions and protons of the same kinetic energy, in order to learn more about the importance of this quantity in determining the pattern of cross sections. Although the proton-induced excitation functions[23] of many nuclides are still changing above 3 GeV, the variation is slow enough to permit interpolation with confidence. The ratios of the heavy-ion cross section to that for protons of the same energy, σ_{HI}/σ_p, are shown in Fig. 5 for each of the present cases. These ratios have an uncertainty of about 25% in their absolute values because of the uncertainty in the calibration of the beam monitor ion chamber, together with the uncertainty in the monitor for the proton cross section measurements. However, this uncertainty affects all of the ratios for a given projectile by the same factor without altering their relative values.

As discussed in the Introduction, the factorization hypothesis applied to these ratios would predict that they should be equal to the ratio of total

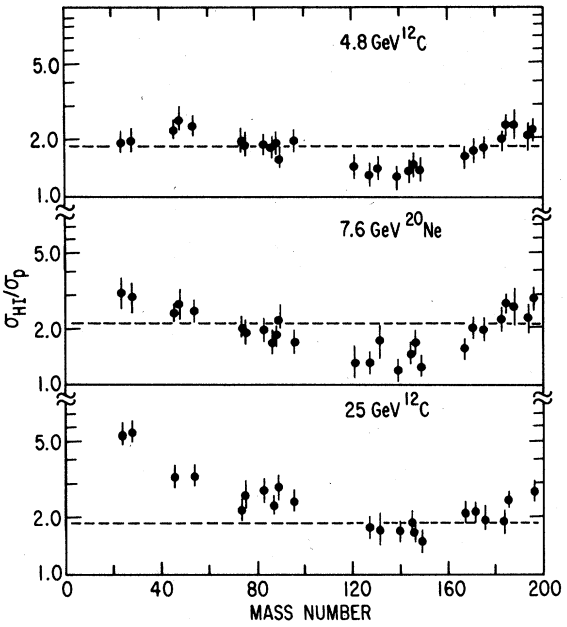

FIG. 5. Ratios of cross sections for production of individual nuclides by heavy-ion projectiles and protons of the same kinetic energy (σ_{HI}/σ_p). The dashed lines indicate the calculated ratio of total reaction cross sections.

reaction cross sections. The dashed lines in Fig. 5 show this ratio for each case; the "soft-spheres" model of Karol[35] was used to calculate the reaction cross sections. The striking feature of these data is the extent to which factorization is obeyed over such a large range of product masses. For 4.8 GeV ^{12}C, the cross section ratios for all nuclides from ^{24}Na to ^{196}Au lie within a factor of 1.5 above or below the reaction cross section ratio. This is probably within the uncertainty limits due to both the absolute cross section measurements and the calculation of the reaction cross sections. The spread is larger for the higher energy heavy ions, and in particular for 25-GeV ^{12}C, there is a strong enhancement for the lightest nuclides.

In addition to the deviation from factorization for these light nuclides, one can see a similar variation in the cross section ratio with product mass number for all three projectiles in Fig. 5. As one proceeds from the near-target heavy nuclides to lighter products, the cross section ratio at first decreases, and reaches a minimum in the mass range $120 \lesssim A \lesssim 150$. For still lighter products the ratio increases, especially for the higher energy projectiles. These changes themselves are indicative of deviations from exact factorization, independent of the absolute cross section uncertainties.

The variation of the σ_{HI}/σ_p ratio with product mass number shown in Fig. 5, and its energy dependence for the three projectiles, suggests a possible correlation with reaction mechanisms. If the yield of the light products is enhanced for heavy-ion projectiles relative to protons, it may be the case that they are formed at the expense of the products which are apparently depleted, namely those in the mass range $120 \lesssim A \lesssim 150$. This could come about if the breakup of highly excited heavy nuclei into two or more light fragments were more probable for heavy-ion than for proton interactions. However, the interpretation of the cross section ratios σ_{HI}/σ_p is not that straightforward. For example, one sees that the light product enhancement increases markedly with projectile kinetic energy, while the heavy product depletion is similar for all three cases. Moreover, the ratios shown were calculated at the same projectile kinetic energy in order to illustrate the importance of that quantity in influencing cross sections. In an energy region where cross sections are still changing, the ratios are sensitive to relatively small differences in the shapes of the excitation functions which may be of no fundamental significance. Thus, any interpretation of the curves in Fig. 5, as indicated above, must be recognized as suggestive and tentative only. Data on fragment correlations are required for a more definitive interpretation of reaction mechanisms.

The scaling of target fragmentation cross sections with reaction cross sections has been previously observed for Cu bombarded with 80-GeV ^{40}Ar ions,[10] for Ag bombarded with 25-GeV ^{12}C ions,[12] and for Ta and Au bombarded with 8.0-GeV ^{20}Ne ions.[14] In each case, the lightest products were observed to have enhanced yields for the heavy-ion projectile as compared to protons. From calculations based on the abrasion-ablation model[36,37] one can correlate, in an approximate way, the impact parameter of a collision with the mass number of the fragment. Thus, near-target residues are formed in peripheral reactions, while the lightest fragments are assumed to be the result of nearly central collisions. In this view, it is not surprising that factorization should break down for such central collisions and one should observe larger yields of these light fragments for heavy-ion projectiles.

The present results thus confirm the previous studies[8-16] by demonstrating the close similarity of the product mass-yield distribution for heavy ions in the multi-GeV energy range and protons of the same energy. The only significant dif-

ference is the higher yield of light nuclides found for the heavy-ion projectiles, as compared to protons, which has been attributed to contributions from central collisions.

A nuclide of special significance in these measurements is ^{196}Au, which is the product formed by the loss of a single neutron from the target. It is well known[38] that the cross sections of such products formed by incident protons, in the (p,pn) reaction, are independent of energy above several hundred MeV and are nearly independent of target mass above $A \approx 60$. This is true in particular for the ^{197}Au$(p,pn)^{196}$Au reaction,[23] which has a constant cross section of about 75 mb above 200 MeV. In projectile fragmentation of relativistic ^{12}C and ^{16}O on various target nuclei, the cross sections of fragments involving the loss of one nucleon from the projectile were found to be enhanced for high-Z targets.[39] This effect was explained in terms of Coulomb dissociation of the projectile by the Coulomb field of the target. The inverse process might be expected to occur for a relativistic heavy-ion projectile, which would lead to enhanced yields of a nuclide such as ^{196}Au from a ^{197}Au target. However, from the systematics shown in Fig. 5, there is no evidence of such an effect outside the experimental errors, since the cross section ratios for ^{196}Au are not greatly different than those of other near-target nuclides. The systematics of the Coulomb dissociation effect[39] indicate that a projectile of higher charge ($Z \gtrsim 30$) would be required for such an effect to become probable.

B. Recoil properties

The recoil velocities due to the initial step of the reaction, $\beta_{\parallel}$, for the three projectiles are shown in Fig. 6 as a function of the nuclide mass number. For comparison, the general trend of the values of $\beta_{\parallel}$ for protons of 3 GeV and 28 GeV energy are shown as the full and dashed curves, respectively. As was previously reported,[19] the data for 25-GeV ^{12}C and 28-GeV protons are essentially the same. In contrast, the $\beta_{\parallel}$ values for fragments formed by 3 GeV protons are larger in magnitude. This was interpreted[19] as indicating that the limiting-fragmentation region for these products has been reached for 2.1 A GeV ^{12}C ions. It is noteworthy that kinetic energy, rather than velocity, seems to be the significant parameter for comparing different projectiles, as is also the case for cross sections (see the preceding section).

The new data presented here are for the lower energy projectiles, which yield products with $\beta_{\parallel}$ values appreciably larger than those of 1–3 GeV protons (although not shown in Fig. 6, the results

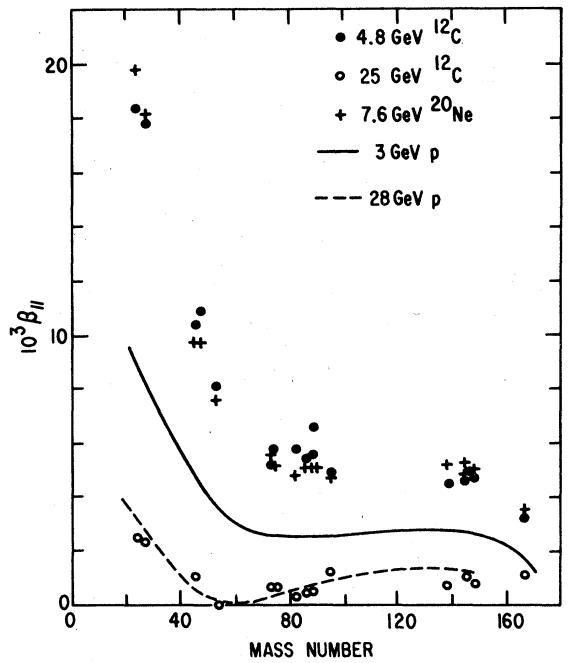

FIG. 6. Variation of $\beta_{\parallel}$, the forward component of the velocity imparted during the first (abrasion) step of the reaction. Points are for heavy ion projectiles, smooth curves show the dependence of A for 3- and 28-GeV protons.

for 1-GeV protons are similar to those for 3-GeV protons). This type of change was also noted in the track-detector measurements of Katcoff and Hudis[17] of fission-fragment angular distributions. They found considerably larger F/B ratios for 2–3 GeV ^{14}N projectiles than at 29 GeV, suggesting that the momentum transferred to the target nucleus decreases with increasing projectile energy. Thus there appears to be a consistent energy dependence of the amount of forward peaking exhibited by target fragments from the interactions of projectiles from protons to ^{20}Ne ions with heavy targets. In all cases studied, there is a decrease of such forward peaking with increasing projectile energy above several GeV.

Although there have not been any measurements of angular distributions for these products in relativistic heavy-ion bombardments, such measurements have been made for proton interactions. The general trend observed for a variety of nuclides formed from proton bombardment of heavy targets[26,40–47] is that the laboratory angular distributions are forward-peaked at energies of 3–6 GeV, and change to sideward peaking above about 10 GeV. At the highest energy studied, 400 GeV,[47] the laboratory angular distributions are peaked at 90° to the beam, and many nuclides actually exhibit a backward enhancement, that is,

higher integrated intensity in the backward hemisphere than in the forward hemisphere. The decrease in $\beta_\parallel$ with increasing projectile energy for heavy ions, which takes place over a similar energy range as these phenomena do for protons, suggests that the underlying cause may be the same, that is, a change in angular distributions from forward to sideward peaked. If this were confirmed by measurements of angular distributions as a function of projectile energy for a variety of projectiles, the hypotheses of factorization and limiting fragmentation would be dramatically confirmed.

In the analysis of the angular and energy distributions measured for protons of 3–6 GeV,[40–44] it was found that the angular distribution of the second step velocity V was not symmetric around 90° in the system moving with velocity $v_\parallel$, but was forward-peaked. This anisotropy invalidates the simple model used here to analyze the thick-target recoil data, which assumes that the forward peaking observed in the laboratory is the result only of the forward component of v, namely $v_\parallel$. If such anisotropies were also present for the heavy-ion projectiles, the values of $\beta_\parallel$ given in Table III would be too large. In any case, however, whether the angular distribution of V is forward peaked or $\beta_\parallel$ is large, the observed result is a large net forward emission in the laboratory at energies of about 400 A MeV. The contrast with the considerably smaller forward peaking for 2.1 A GeV ^{12}C ions shows that the region of limiting fragmentation has not been reached at energies of 400 A MeV. It has been suggested[27] that a projectile velocity of $\beta = 0.9$ might be a reasonable lower limit for the onset of limiting fragmentation, since further increases in projectile velocity would change the interaction time by less than 10%. At an energy of 400 A MeV, the projectile velocity is $\beta = 0.71$, and thus limiting behavior might not be expected, while $\beta = 0.95$ at an energy of 2.1 A GeV, and thus one should expect limiting fragmentation to hold.

The magnitudes of the $\beta_\parallel$ values shown in Fig. 6 are only a small fraction of the projectile β, even for the light nuclides at 400 A MeV. This is consistent with their identification as target fragmentation products; in other words, they have small velocities relative to the target rest frame. It is somewhat surprising that projectiles of different masses but nearly the same velocities (4.8-GeV ^{12}C and 7.6-GeV ^{20}Na) should form products with essentially identical $\beta_\parallel$ values over such a wide mass range.[48] Moreover, similar $\beta_\parallel$ values were found for the target fragments of Ta bombarded with 8.0-GeV ^{20}Ne ions,[27] demonstrating a target independence over the mass number range $A = 181$–197. A smooth dependence of $\beta_\parallel$ on the projectile rapidity ($y = \tanh^{-1}\beta$) for the nuclides ^{24}Na and ^{28}Mg formed from a Cu target by protons, ^{4}He, and ^{12}C ions has been found.[18] This does not appear to be the case for heavy targets, since the $\beta_\parallel$ values are quite different for protons of 1–3 GeV and ^{12}C of 25 GeV, with nearly the same projectile rapidity. The projectile kinetic energy appears to be the proper scaling variable in the latter case.

In all systems where the dependence of $\beta_\parallel$ for target fragments on projectile energy has been studied, a decrease of $\beta_\parallel$ with increasing energy above a few GeV is observed.[48] For the present system of a heavy target, the rate of decrease for ^{12}C projectiles, although based on only two energies, is much more rapid than that for protons. This is the case whether one uses kinetic energy or rapidity as the independent variable. A treatment of this problem has recently been proposed by Cumming,[49] based on the collective tube model.[50] In this model the target nucleons which lie in the path of a relativistic projectile are considered to act collectively and are treated as an effective target. A linear dependence of $\beta_\parallel$ on E^{-1} is predicted,[49] where E is the *total* energy of the projectile, and the slope of the line is proportional to Δm, the mass of the effective target. Data for two proton-induced reactions were shown to follow this dependence above kinetic energies of 2–3 GeV. In order to learn whether this is also the case for heavy ions, data would be needed at more energies, since two points are not sufficient to establish the predicted E^{-1} dependence. The larger slope found here for ^{12}C suggests a larger value of Δm, as might be expected for a heavy ion as compared to a proton.

The velocity imparted to the product nucleus by the second step of the reaction (the ablation, or deexcitation step) is expected to be less sensitive to the details of the initial interaction. In the case of proton bombardments, for which the most data are available, the primary factor influencing the magnitude of this velocity is the relative contributions of fission and evaporation to the deexcitation. For medium-mass nuclides the mechanism changes from fission at bombarding energies of several hundred MeV to deep spallation above about 6 GeV, as shown by the drastic change in the mass-yield curve (Fig. 3). In this same energy range the second-step velocities decrease by about a factor of 2, as the fission contribution to the cross section decreases.[25] It is clear from the cross sections reported above that there is no sign of a separate fission peak for these heavy-ion energies, and hence we expect that the second-step velocities will be similar to those of proton-

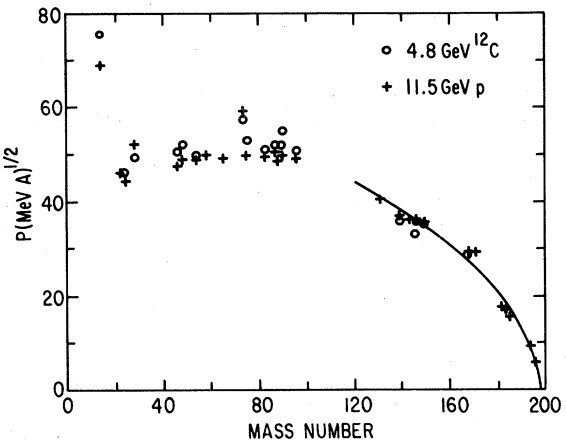

FIG. 7. Dependence of P, the mean momentum imparted by the second (ablation) step, on fragment mass number, for 4.8 GeV ^{12}C (○) and 11.5-GeV p (+). The curve shows the $\sqrt{\Delta A}$ behavior for $\Delta A < 70$ ($\Delta A = A_{\text{target}} - A_{\text{product}}$).

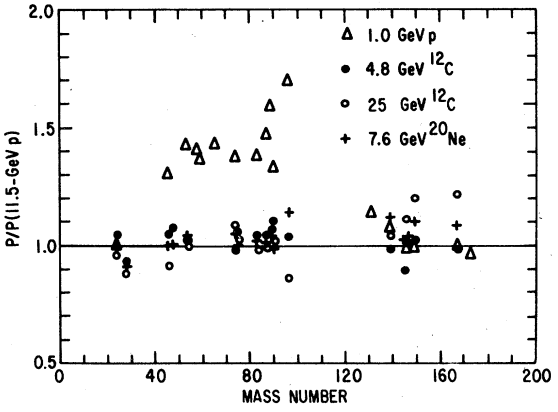

FIG. 8. Ratios of the fragment mean momentum to that for 11.5-GeV protons.

induced fragments above 6 GeV.

This is in fact the case, as is shown by the comparison of the mean momentum, $P = AV$, as a function of mass number for 11.5-GeV protons[25] and 4.8-GeV ^{12}C shown in Fig. 7. The nuclides corresponding to a mass loss from the target, ΔA, of up to about 70 mass numbers, exhibit a smooth increase of P with increasing ΔA. This increase is well approximated by $P \propto \sqrt{\Delta A}$, shown by the curve in Fig. 7, and is indicative of the random addition of momentum increments imparted to the nucleus by evaporation during the deexcitation steps. Below $A = 100$ the recoil momentum becomes nearly constant for the nuclides studied here, which have only a small contribution of a fission mechanism to their formation.

The similarity of these momenta to those of products formed by protons of 11.5 GeV energy, and the difference from those of much lower energy, is shown in Fig. 8. Here we plot the ratio of mean momentum for each projectile to that found for 11.5 GeV protons. These are within about 20% of unity for the three heavy-ion projectiles. The ratios for 1.0-GeV protons are larger in the mass range $46 \leq A \leq 96$, varying from 1.3 to 1.7, depending on the nuclide. For a light nuclide, such as ^{24}Na, there is very little change in momentum with proton energy, as is also the case for the spallation products of $A > 130$. There seems to be a tendency for the momenta of the heaviest nuclides formed by 25-GeV ^{12}C ions to be significantly larger than those of the same nuclides formed by 11.5-GeV protons, but additional data would be needed to confirm this.

The general picture which these comparisons have shown is that the second step of the reaction (ablation or evaporation) is similar for heavy ions and protons of about the same kinetic energy, but not for projectiles of the same velocity. The velocity imparted to the target by the first step, however, is much larger for heavy ions of energy ~400 A MeV than for protons of any energy. This is model-dependent in that these velocities are derived assuming an angular distribution for emitting the final product nucleus, which is isotropic in the moving system. If this assumption is incorrect, as it is for protons below 10 GeV,[40-44] one can still state that the extent of forward emission of target fragments is much larger for the heavy ions than for protons. This leaves open the question of what proportion is due to emission from a moving source and what to a forward-peaked angular distribution. At a higher energy of 2.1 A GeV, however, all of the observed properties of the target fragments from ^{12}C bombardment are similar to those of fragments from bombardment by protons of about the same energy.

V. SUMMARY AND CONCLUSIONS

The cross-section measurements reported here have extended and confirmed previous results[8-16] on target fragmentation which showed the relative cross sections to be nearly independent of projectile mass and energy for energies above a few GeV. This was taken as evidence in support of the limiting fragmentation hypothesis at these energies. The fact that the cross sections appear to scale with the total reaction cross section is evidence that factorization also applies to these fragments. The only exception is for light nuclides, such as ^{24}Na, which have enhanced yields

as compared to proton-induced reactions and whose cross sections are increasing between 0.4 A GeV and 2.1 A GeV. This has been taken as evidence that the more nearly central collisions are contributing to the light products, but not to the heavier ones, which are formed in peripheral collisions.

The recoil measurements, in contrast to the above results, show large changes over the same energy range. At energies near 0.4 A GeV the target fragments have large F/B ratios, larger than those observed for protons of any energy. This preferential forward emission is interpreted in terms of the standard two-step model as arising from isotropic emission from a source moving in the forward direction. If the emission were anisotropic, having a forward-peaked angular distribution as has been inferred for proton-induced reactions below 10 GeV, this would also lead to large F/B ratios. More detailed measurements of angular distributions and energy spectra as a function of angle are needed to elucidate this question. In either case, however, the results show that factorization is not applicable at energies of 0.4 A GeV, since the fragments formed by heavy ions and protons have such different kinematic behavior. Limiting fragmentation has also not been attained, as evidenced by the large changes in the F/B ratios when the projectile energy increases from 0.4 to 2.1 A GeV.

The fragment recoil behavior for 2.1 A GeV ^{12}C ions, however, does appear to be consistent with both factorization and limiting fragmentation. This is deduced from the close similarity of those data with that for protons of the same kinetic energy, and by the fact that there is almost no change when the proton kinetic energy is increased by an order of magnitude to 300 GeV. It is clearly desirable to obtain such data for the same projectile (^{12}C) at intermediate energies between the two reported in this work, in order to learn what the energy or velocity dependence of these kinematic quantities is. It would then be possible to test theories of the reaction mechanism, such as the collective tube model prediction[49] of a linear dependence of $\beta_{\parallel}$ on E^{-1}.

ACKNOWLEDGMENTS

We wish to thank W. Everette and F. Lothrop for their assistance in obtaining the target bombardments at the Bevalac, and D. Morrissey for help during the bombardments. This research was performed under the auspices of the Office of Basic Energy Sciences, Division of Nuclear Physics, U. S. Department of Energy.

[1]For a recent review of this topic, see A. S. Goldhaber and H. H. Heckman, Annu. Rev. Nucl. Part. Sci. 28, 161 (1978).
[2]H. H. Heckman, H. J. Crawford, D. E. Greiner, P. J. Lindstrom, and L. W. Wilson, Phys. Rev. C 17, 1651 (1978).
[3]A. M. Poskanzer, R. G. Sextro, A. M. Zebelman, H. H. Gutbrod, A. Sandoval, and R. Stock, Phys. Rev. Lett. 35, 1701 (1975).
[4]J. Gosset, H. H. Gutbrod, W. G. Meyer, A. M. Poskanzer, A. Sandoval, R. Stock, and G. D. Westfall, Phys. Rev. C 16, 629 (1977).
[5]See the review by H. Bøggild and T. Ferbel, Annu. Rev. Nucl. Sci. 24, 451 (1974).
[6]D. E. Greiner, P. J. Lindstrom, H. H. Heckman, B. Cork, and F. S. Bieser, Phys. Rev. Lett. 35, 152 (1975).
[7]P. J. Lindstrom, D. E. Greiner, H. H. Heckman, B. Cork, and F. S. Bieser, Lawrence Berkeley Laboratory Report No. LBL 3650, 1975 (unpublished).
[8]J. B. Cumming, P. E. Haustein, R. W. Stoenner, L. Mausner, and R. A. Naumann, Phys. Rev. C 10, 739 (1974).
[9]J. B. Cumming, R. W. Stoenner, and P. E. Haustein, Phys. Rev. C 14, 1554 (1976).
[10]J. B. Cumming, P. E. Haustein, T. J. Ruth, and G. V. Virtes, Phys. Rev. C 17, 1632 (1978).
[11]C. R. Rudy and N. T. Porile, Phys. Lett. 59B, 240 (1975).
[12]N. T. Porile, G. D. Cole, and C. R. Rudy, Phys. Rev. C 19, 2288 (1979).
[13]D. J. Morrissey, W. Loveland, and G. T. Seaborg, Z. Phys. A 289, 123 (1978).
[14]D. J. Morrissey, W. Loveland, M. de Saint Simon, and G. T. Seaborg, Phys. Rev. C 21, 1783 (1980).
[15]W. Loveland, R. J. Otto, D. J. Morrissey, and G. T. Seaborg, Phys. Lett. 69B, 284 (1977).
[16]W. Loveland, R. J. Otto, D. J. Morrissey, and G. T. Seaborg, Phys. Rev. Lett. 39, 320 (1977).
[17]S. Katcoff and J. Hudis, Phys. Rev. C 14, 628 (1976).
[18]J. B. Cumming, P. E. Haustein, and H. -C. Hseuh, Phys. Rev. C 18, 1372 (1978).
[19]S. B. Kaufman, E. P. Steinberg, and B. D. Wilkins, Phys. Rev. Lett. 41, 1359 (1978).
[20]J. D. Bowman, W. J. Swiatecki, and C. F. Tsang, Lawrence Berkeley Laboratory Report No. LBL-2908, 1973 (unpublished).
[21]J. Hüfner, K. Schäfer, and B. Schürmann, Phys. Rev. C 12, 1888 (1975).
[22]S. B. Kaufman, M. W. Weisfield, E. P. Steinberg, B. D. Wilkins, and D. Henderson, Phys. Rev. C 14, 1121 (1976).
[23]S. B. Kaufman and E. P. Steinberg, Phys. Rev. C 22, 167 (1980).
[24]S. B. Kaufman and M. W. Weisfield, Phys. Rev. C 11, 1258 (1975).
[25]S. B. Kaufman, E. P. Steinberg, and M. W. Weisfield, Phys. Rev. C 18, 1349 (1978).

[26]J. A. Urbon, S. B. Kaufman, D. J. Henderson, and E. P. Steinberg, Phys. Rev. C 21, 1048 (1980).
[27]W. Loveland, D. J. Morrissey, K. Aleklett, G. T. Seaborg, S. B. Kaufman, E. P. Steinberg, B. D. Wilkins, J. B. Cumming, P. E. Haustein, and H. C. Hseuh, Phys. Rev. C (to be published).
[28]W. Everette, private communication.
[29]N. Sugarman, M. Campos, and K. Wielgoz, Phys. Rev. 101, 388 (1956).
[30]N. T. Porile and N. Sugarman, Phys. Rev. 107, 1410 (1957).
[31]N. Sugarman, H Münzel, J. A. Panontin, K. Wielgoz, M. V. Ramaniah, G. Lange, and E. Lopez-Menchero, Phys. Rev. 143, 952 (1966).
[32]J. M. Alexander, in *Nuclear Chemistry*, edited by L. Yaffe (Academic, New York, 1968), Vol. I, p. 273; L. Winsberg and J. M. Alexander, *ibid.*, p. 340.
[33]L. Winsberg, Nuclear Instrum. Methods 150, 465 (1978).
[34]L. C. Northcliffe and R. F. Schilling, Nucl. Data A7, 233 (1970).
[35]P. J. Karol, Phys. Rev. C 11, 1203 (1975).
[36]D. J. Morrissey, W. R. Marsh, R. J. Otto, W. Loveland, and G. T. Seaborg, Phys. Rev. C 18, 1267 (1978).
[37]L. F. Oliveira, R. Donangelo, and J. O. Rasmussen, Phys. Rev. C 19, 826 (1979).
[38]J. R. Grover and A. A. Caretto, Annu. Rev. Nucl. Sci. 14, 51 (1964).
[39]H. H. Heckman and P. J. Lindstrom, Phys. Rev. Lett. 37, 56 (1976).
[40]J. B. Cumming, R. J. Cross, Jr., J. Hudis, and A. M. Poskanzer, Phys. Rev. 134, B167 (1964).
[41]A. M. Poskanzer, G. W. Butler, and E. K. Hyde, Phys. Rev. C 3, 882 (1971).
[42]E. K. Hyde, G. W. Butler, and A. M. Poskanzer, Phys. Rev. C 4, 1759 (1971).
[43]R. G. Korteling, C. R. Toren, and E. K. Hyde, Phys. Rev. C 7, 1611 (1973).
[44]G. D. Westfall, R. G. Sextro, A. M. Poskanzer, A. M. Zebelman, G. W. Butler, and E. K. Hyde, Phys. Rev. C 17, 1368 (1978).
[45]L. P. Remsberg and D. G. Perry, Phys. Rev. Lett. 35, 361 (1975).
[46]D. R. Fortney and N. T. Porile, Phys. Lett. 76B, 553 (1978).
[47]N. T. Porile, D. R. Fortney, S. Pandian, R. A. Johns, T. Kaiser, K. Wielgoz, T. S. K. Chang, N. Sugarman, J. A. Urbon, D. J. Henderson, S. B. Kaufman, and E. P. Steinberg, Phys. Rev. Lett. 43, 918 (1979).
[48]It has been pointed out by the referee of this paper that this result is consistent with the prediction of the two-step model of Masuda and Uchiyama [Phys. Rev. C 15, 1598 (1977)] and is a consequence of the kinematics only. See also Ref. 1, p. 185.
[49]J. B. Cumming, Phys. Rev. Lett. 44, 17 (1980).
[50]G. Berland, A. Dar, and G. Eilam, Phys. Rev. D 13, 161 (1976); Meng Ta-Chung, *ibid.* 15, 197 (1977).